Wideband RF photonic in-phase and quadraturephase generation

Emami, Hossein; Sarkhosh, Niusha; Bui, Lam; Mitchell, Arnan

Emami, Sarkhosh, N., Bui, L., & Mitchell, A. (2008). Wideband RF photonic in-phase and quadraturephase generation. Optics Letters, 33(2), 98–100. https://doi.org/10.1364/OL.33.000098
Document Version: Published Version

Published Version: https://doi.org/10.1364/OL.33.000098

Citation:
Emami, H, Sarkhosh, N, Bui, L and Mitchell, A 2008, 'Wideband RF photonic in-phase and quadrature-phase generation', Optics Letters, vol. 33, no. 2, pp. 98-100.

Wideband RF photonic in-phase and quadrature-phase generation

Hossein Emami,* Niusha Sarkhosh, Lam Anh Bui, and Arnan Mitchell

Microelectronics and Materials Technology Center, School of Electrical and Computer Engineering, RMIT University, GPO BOX 2476V, Melbourne, 3001, Victoria, Australia
**Corresponding author: hossein.emami@rmit.edu.au*

Received August 31, 2007; revised November 20, 2007; accepted November 29, 2007;
posted December 3, 2007 (Doc. ID 87097); published January 3, 2008

A photonic implementation of a practical broadband RF Hilbert transformer is demonstrated by using a four-tap transversal system. An almost ideal 90° phase shift with less than 3 dB of amplitude ripple has been achieved from 2.4 to 17.6 GHz. An efficient method to realize both transformed (quadrature-phase) and reference (in-phase) signal has been achieved by using a coarse wavelength division multiplexing coupler. Extension of the transformer bandwidth and further improvements of its implementation are discussed.

OCIS codes: 060.5625, 060.2360, 070.6020, 350.4010.

Photonic processing of microwave signals has received significant attention in the past two decades in an attempt to remove the bandwidth bottlenecks incurred in conventional electronics. This interest has generated the research area known as microwave photonics [1]. Microwave photonics is especially suitable for broadband signal processing. The other advantages include immunity to electromagnetic interference and the ability to provide parallel processing of signals and flexible configurability. Many microwave photonic systems have been proposed and demonstrated over the years, including tunable and shape reconfigurable [2–5] filters and phased-array beam formers [6].

In some applications the signal phase is of critical importance, for instance, vector modulation [7], single-sideband modulation [8], and frequency measurement [9]. In these latter applications, access to both in-phase and quadrature-phase (90°) versions of the signal is necessary. Two orthogonally phased components provide an additional degree of flexibility and versatility for signal processing.

There are several techniques to generate in-phase and quadrature-phased components of an RF signal. The most popular technique utilizes 90° hybrid couplers. Alternatively, the orthogonal phase component could be generated by using the Hilbert transformation. An electrical implementation of a Hilbert transformer has been demonstrated [10]. It is evident from the reported results that the responses of both the electrical hybrid coupler and the electrical Hilbert transformer were characterized by large phase and amplitude ripple due to significant dispersion existing within the microwave circuits.

A photonic approach to implement an RF Hilbert transformer that exhibits minimum microwave dispersion and achieves close to an ideal response has recently been proposed [11]. In this Letter, a practical implementation of a RF photonic Hilbert transformer has been presented in which much improvement of bandwidth and phase response has been achieved compared with [10]. Furthermore, no network matching is needed, and there is flexibility for dynamically adjusting passband ripple and bandwidth.

The frequency response of an ideal Hilbert transform is $-j\,\mathrm{sgn}(\omega)$, which exhibits a 90° frequency-independent phase shift. The impulse response associated with this transform is $1/(\pi t)$. This impulse response extends infinitely in time and must be truncated in practice. In addition, the impulse response exhibits negative time; therefore practical implementation of the Hilbert transformer would require a reference that is delayed with respect to the transformed components as shown in Fig. 1 (inset). The continuous time impulse response must also be sampled by discrete taps. An appropriate window function, for instance, a Kaiser windowing function [12], should be applied to the taps to minimize the Gibbs effect caused by truncation. In practice the window used can be manipulated to optimally trade off ripple and bandwidth [11,12]. Having chosen a finite number of discrete taps, exact tap weights are obtained by sampling the windowed Hilbert transform.

To allow tap weights and spacing to be chosen, the Hilbert transformer specifications must be defined.

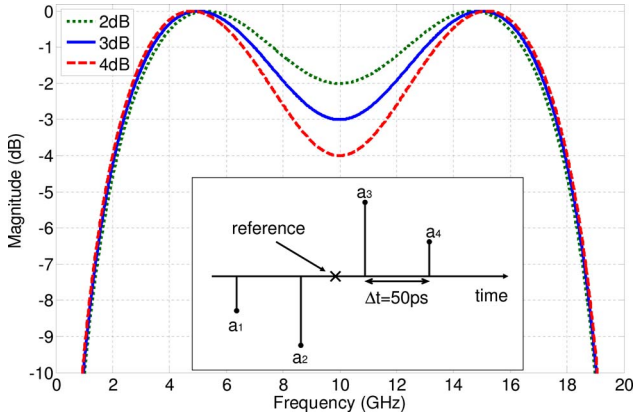

Fig. 1. (Color online) Magnitude of impulse response of a four-tap system.

The specification for this design were set as bandwidth 2.5–17.5 GHz and passband ripple of amplitude ≤3 dB and phase ≤5°. To simplify the demonstration, the design was limited to a transversal system of four taps equally spaced in time. For the bandwidth of 2.5–17.5 GHz, the first null of the transversal system was placed at 20 GHz, associated with a tap spacing of 1/(20 GHz), or 50 ps. The tap weights were adjusted to apply an appropriate window function. In this case, as there were only four taps, the optimization was achieved empirically to achieve the designated ripple and bandwidth. As the impulse response has odd symmetry with the two center taps having the largest amplitude, normalizing the tap weights with respect to the center tap amplitude, the tap weights of the two center taps are always $a_3=-a_2=1$. The weights of the remaining two taps could be chosen to achieve various levels of passband ripple. The system frequency response was computed by taking the Fourier transform of the impulse response. Figure 1 presents the amplitude response with passband ripples of 2, 3, and 4 dB. The phase response of the three cases of Fig. 1 remained ideal, since the impulse response always has odd symmetry. It is evident from Fig. 1 that the Hilbert transform with 3 dB of ripple meets the set design specification, which results in $a_4=-a_1=0.3328$ and $a_3=-a_2=1$ [11].

Having specified tap weights and spacing, the system was then implemented as shown in Fig. 2. Using a wavelength division multiplexing (WDM) technique, taps a_1–a_4 were associated with optical wavelengths λ_1–λ_4, respectively. Since the impulse response has odd symmetry, both positive and negative tap coefficients must be implemented.

The wavelengths were divided into two groups of two each. For the first group, λ_1 and λ_2 were combined by using a 3 dB optical coupler and were modulated by using a Mach–Zehnder modulator (MZM) biased at quadrature with negative slope (V^-). Similarly, for the second group, λ_3 and λ_4 were combined and modulated with positive slope (V^+) [2,4]. The RF signal was fed equally to both modulators through a broadband Wilkinson power divider. All wavelength channels were then combined. Variable optical lengths (VOL1 and VOL2) were used after the modulators to ensure that the RF signals carried by the wavelengths were subjected to the same delay.

Figures 2(a) and 2(b) show the wavelengths with assigned tap weights. As can be seen, the first wavelength (λ_1) had two components. The portion that is shown by a solid line was used as tap a_1 of the transversal system, while the other portion (dotted line) was used as the system reference. The combined output consisting of four taps is shown in Fig. 2 inset (c). This output was transmitted through a dispersive fiber, where each wavelength experienced a different delay and hence produced taps at different respective times. The dispersed signal was then amplified by using an erbium-doped fiber amplifier (EDFA) to overcome the system loss.

By use of a coarse WDM coupler (CWDM), approximately 90% of the signal at λ_1 was separated and used as the system reference. Figure 2 insets (d) and (e) show the optical spectrum at Port 1 and Port 2 of the CWDM. At Port 1 all wavelengths λ_{1-4} are present, while at Port 2 only the λ_1 component is present. VOL3 and VOL4 were used to time shift the signal at Port 2 to be placed exactly at the middle of the four-tap set before being detected by a photodetector. This became the system reference. This time-shift concept is illustrated in Fig. 2 inset (f). Having obtained the correct tap positions, we tuned the tap amplitudes to $a_4=-a_1=0.3328$ and $a_3=-a_2=1$ by carefully adjusting the laser powers.

With a 2.354 km of single-mode fiber as a dispersive medium with a fiber dispersion of 17 ps/(nm km), the separation between wavelength channels was computed to be 1.25 nm to produce a tap spacing of 50 ps. We chose $\lambda_1=1543.94$ nm to match the splitting wavelength of the CWDM. Wavelengths λ_2–λ_4 were selected as 1545.19, 1546.44, and 1547.69 nm. Since the dispersion was not exactly linear and nontrivial dispersion was also contributed by other system components, the actual wavelengths for λ_2 and λ_3 were empirically adjusted to 1545.3 and 1546.59 nm.

A vector network analyzer was used to characterize the system response. The vector network analyzer was calibrated with respect to reference output Out 2 and then used to measure the amplitude and phase response of Out 1. These results are presented in Fig.

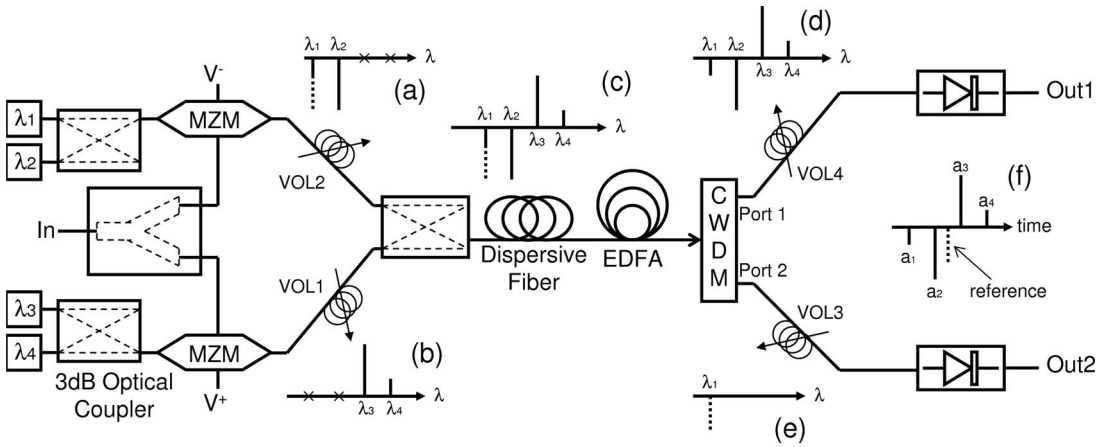

Fig. 2. System implementation.

3, together with the calculated responses for the 3 dB ripple case of Fig. 1 for easy comparison. Excellent agreement between the measurement and simulation is evident. An amplitude variation of ≤3 dB was achieved between 2.4 and 17.6 GHz, and an almost ideal 90° phase response with ≤5° deviation was obtained for all frequencies. An increment of amplitude and phase uncertainty was observed near the system null at 20 GHz. This degradation, however, occurred outside the nominal system bandwidth. It was thus concluded that implemented system in fact behaves as theoretically predicted.

Further simplification of the implementation is possible. Replacing the two oppositely biased modulators with a single balanced MZM could eliminate the need for a RF power divider [2,4]. This would also simplify path length equalization and reduce component count and optical splitting losses.

This photonic implementation offers the flexibility of a customized passband response where the passband ripple and the bandwidth can be dynamically configured by changing the tap weights and the wavelength spacing. It also exhibits graceful degradation outside the 3 dB bandwidth. As the MZMs' input and the photodetectors' output have a 50 Ω impedance, no matching network was needed. It would be desirable to extend the system bandwidth to 2–40 GHz with less than 3 dB of ripple. Further improvement of bandwidth and ripple could be achieved by employing extra taps as suggested in [11]. Implementations of these improvements are currently under investigation.

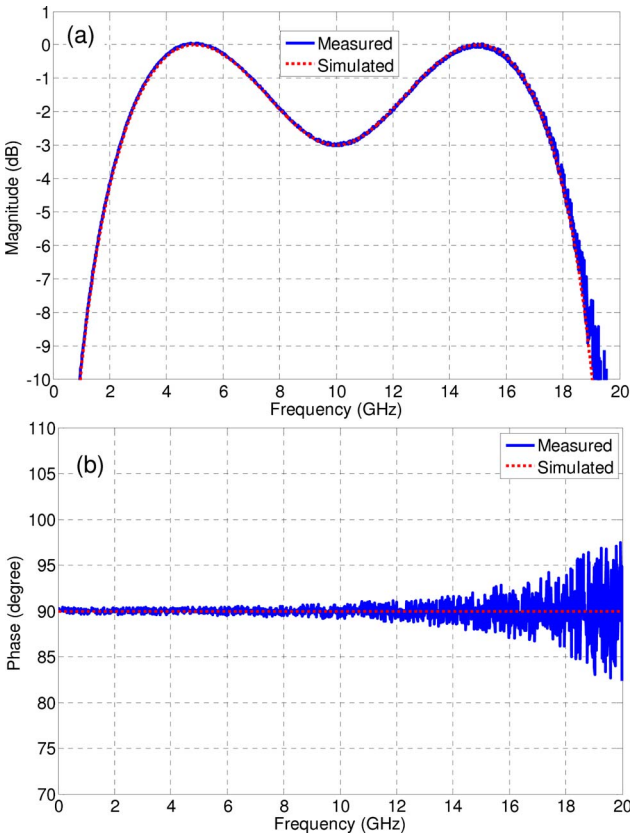

Fig. 3. (Color online) Measured and simulated system response: (a) magnitude, (b) phase.

In conclusion, a broadband Hilbert transformer was demonstrated by using a photonic transversal signal processing scheme. Efficient use of CWDM enables both transformed (quadrature-phase) and reference (in-phase) signals to be produced. Both system bandwidth and passband ripple can be customized and dynamically configured. No matching network is needed. Suggestions for extension of the bandwidth to 2–40 GHz and further improvements of the implementation were proposed. This Hilbert transformer is suitable for in-phase and quadrature-phase optical processing of broadband microwave signal applications.

References

1. A. J. Seeds and K. J. Williams, J. Lightwave Technol. **24**, 4628 (2006).
2. R. A. Minasian, IEEE Trans. Microwave Theory Tech. **54**, 832 (2006).
3. D. B. Hunter and L. V. T. Nguyen, IEEE Trans. Microwave Theory Tech. **54**, 900 (2006).
4. J. Capmany, B. Ortega, and D. Pastor, J. Lightwave Technol. **24**, 201 (2006).
5. B. Vidal, V. Polo, J. L. Corral, and J. Marti, Electron. Lett. **39**, 547 (2003).
6. B. Vidal, T. Mengual, C. Ibanez-Lopez, J. Marti, I. McKenzie, E. Vez, J. Santamaria, F. Dalmases, and L. Jofre, IEEE Photon. Technol. Lett. **18**, 1200 (2006).
7. L. A. Bui, A. Mitchell, K. Ghorbani, and T.-H. Chio, IEEE Microw. Wirel. Compon. Lett. **15**, 309 (2005).
8. T. Kawanishi and M. Izutsu, IEEE Photon. Technol. Lett. **16**, 1534 (2004).
9. L. V. T. Nguyen and D. B. Hunter, IEEE Photon. Technol. Lett. **18**, 1188 (2006).
10. C. D. Holdenried, J. W. Haslett, and B. Davies, IEEE Microw. Wirel. Compon. Lett. **15**, 303 (2005).
11. H. Emami, L. A. Bui, and A. Mitchell, in *Proceedings of Asia Pacific Microwave Photonics Conference* (ILCC, 2006), pp. 173–176.
12. J. F. Kaiser and R. W. Schafer, IEEE Trans. Acoust., Speech, Signal Process. **ASSP-28**, 105 (1980).